Rev. Adv. Mater. Sci. 40 (2015) 249-256

MECHANICAL PROPERTIES OF GRAPHENE NANORIBBONS: A SELECTIVE REVIEW OF COMPUTER SIMULATIONS

A.V. Orlov[1,2] and I.A. Ovid'ko[1,2,3]

[1]Research Laboratory for Mechanics of New Nanomaterials, St. Petersburg State Polytechnical University, St. Petersburg 195251, Russia
[2]Institute of Problems of Mechanical Engineering, Russian Academy of Sciences, Bolshoj 61, Vasilievskii Ostrov, St. Petersburg 199178, Russia
[3]Department of Mathematics and Mechanics, St. Petersburg State University, St. Petersburg 198504, Russia

Received: January 11, 2015

Abstract. This paper presents an overview of research efforts focused on computer simulations of unique mechanical properties exhibited by graphene nanoribbons, narrow graphene ribbons with widths lower than 100 nm (typically < 10 nm). A particular attention is devoted to the edge, size and chirality effects on the Young modulus, fracture stress (strength) and strain of graphene nanoribbons. Also, fracture mechanisms are discussed which, according to computer simulations, effectively operate in graphene nanoribbons.

1. INTRODUCTION

Graphene is a special two-dimensional carbon material exhibiting unique electronic, mechanical and thermal properties [1-7]. One of the most effective approaches to modify, design and control its outstanding electronic properties is to fabricate graphene in the form of nanoribbons, narrow graphene ribbons with width < 100 nm (typically < 10 nm) [8-10]. In fact, graphene nanoribbons are viewed as basic elements for a new generation of nanoelectronic devices and nano-electromechanical systems. The edge and associated size and chirality effects come into play in graphene nanoribbons and strongly influence their electronic properties. For instance, following theoretical predictions [11-13], the edge effects can control whether a graphene nanoribbon is metallic, insulating or semiconducting. In addition, elastic strains in graphene nanoribbons dramatically affect their electronic properties and thereby can be used in design and control of these properties; see, e.g., [14,15].

In parallel with the elastic properties of graphene nanoribbons, it is highly important to understand their plastic flow and fracture behaviors. First of all, plastic deformation and fracture processes of graphene nanoribbons are critical for performance and reliability of nanoelectronic and electromechanical devices based on such nanoribbons. Besides, graphene is specified by highest ever measured tensile strength of ≈ 130 GPa [7,16], in which case the basic knowledge on sensitivity of the mechanical properties of graphene nanoribbons to the edge, size and chirality effects are of crucial significance for exploitation of excellent mechanical characteristics of graphene. Up to date, examinations in this area have been limited to computer simulations, because of extraordinarily high difficulties for experimental study of mechanical characteristics of graphene nanoribbons. The main aim of this paper is to give a selective overview of research efforts focused on computer simulations of the unique mechanical properties exhibited by graphene nanoribbons. Also, frac-

Corresponding author: I.A. Ovid'ko, e-mail: ovidko@gmail.com

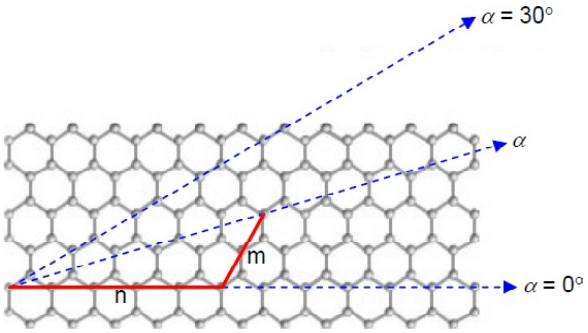

Fig. 1. (Color online) Chirality of graphene nanoribbons is characterized by chirality vector (*m*, *n*) or, in an equivalent way, chirality angle α.

ture mechanisms are discussed which, according to computer simulations, effectively operate in graphene nanoribbons.

2. EDGE, SIZE, AND CHIRALITY EFFECTS ON MECHANICAL PROPERTIES OF GRAPHENE NANORIBBONS: GENERAL ASPECTS

The electronic state of a carbon atom in a carbon nanostructure dramatically depends on the number and arrangement of its neighboring atoms; see, e.g., [17]. As a corollary, the edge effect occurs in graphene nanoribbons, where ratio of the number of edge carbon atoms (located at graphene edges) to that of interior carbon atoms in a nanoribbon is large, as compared to the same ratio characterizing a conventional graphene sheet with large values of both length and width. The size effect in a graphene nanoribbon manifests itself, first of all, through sensitivity of its properties to the nanoribbon width. This effect is evidently associated with the edge effect, because the nanoribbon width is directly related to the number of edge carbon atoms and that of interior carbon atoms.

Besides, the chirality effect occurs in graphene nanoribbons, because geometry of edges influences the electronic states of carbon atoms through arrangement of their neighboring atoms. By analogy with carbon nanotubes, geometry of edges in graphene nanoribbons is specified by a chiral vector (*m*,*n*), where *m* and *n* (<*m*) are integers in the decomposition of the chiral vector into graphene lattice vectors, as shown in Fig. 1. Also, geometry/chirality of a graphene nanoribbon edge is unambiguously characterized by a chirality angle α made by the chirality vector and the zigzag direction (Fig. 1). This angle is in the following relationship with the characteristic integers *m* and *n*: $\alpha = \arctan(3^{1/2} m / (m + n))$ [18]. When $\alpha = 30^{o}$, a nanoribbon edge is pure armchair (Fig. 2a). When $\alpha = 0^{o}$, a nanoribbon edge is pure zigzag (Fig. 2b). When α is in the range $0^{o} < \alpha < 30^{o}$, a nanoribbon edge is of a mixed (zigzag plus armchair) geometry (Fig. 3).

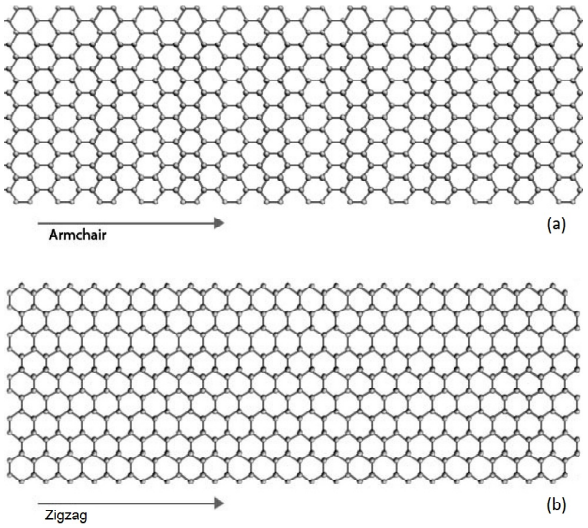

Fig. 2. Graphene nanoribbons having (a) armchair and (b) zigzag edges in longitudinal direction.

In next section, computer simulations will be discussed dealing with the edge, size and chirality effects on mechanical properties of graphene nanoribbons. Also, a particular attention will be devoted to fracture mechanisms operating in graphene nanoribbons.

3. EDGE, SIZE AND CHIRALITY EFFECTS ON MECHANICAL PROPERTIES OF GRAPHENE NANORIBBONS: COMPUTER SIMULATIONS

Zhao with co-workers [19] performed simulations of deformation behaviors exhibited by graphene nanoribbons with various sizes under uniaxial tensile load. The focuses were placed on the size and chirality effects on the elastic properties of graphene nanoribbons in tensile tests. Also, the elastic moduli, the fracture strength (defined as the engineering stress on the material at the breaking point) and the fracture strain of bulk (large-area) graphene under tension tests in armchair and zigzag directions were calculated. The simulation cell in *xy* plane, for bulk graphene, has a square-like shape with width and length being 10.08 nm and 10.22 nm, respectively. Periodic conditions in both *x* and y directions were used. In the case of bulk graphene, in particular, with the molecular dynamics simulations based on the adaptive intermolecular reactive

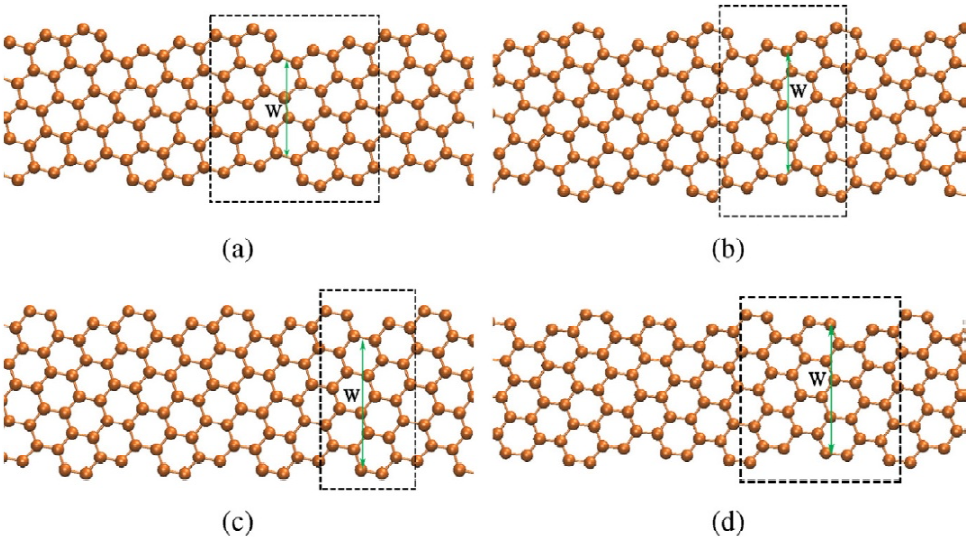

Fig. 3. Graphene nanoribbons with different chirality and their unit cell. (a) $\alpha = 10.89^{o}$; (b) 13.90^{o}; (c) 19.11^{o}; and (d) 23.41^{o}. Reprinted with permission from [A. Tabarraei, S. Shadalou, J.-H. Song, Mechanical properties of graphene nanoribbons with disordered edges. *Computational Materials Science*, Volume 96 (2015) 10-19]. Copyright (2015) Elsevier.

bond order (AIREBO) potential, one finds that Young modulus $Y_b \approx 1.01$ TPa and Poisson ratio $\nu_b \approx 0.21$ [19]. In addition, according to the molecular dynamics simulations [19], the tensile fracture strength σ_t = 90 GPa and the fracture strain $\varepsilon_f = 0.13$ during uniaxial tension of bulk graphene along armchair direction; whereas $\sigma_t = 107$ GPa and $\varepsilon_f = 0.20$ in tensile test along zigzag direction. These results of the simulations are consistent with data [16] obtained in the experiment concerning a circle-like graphene membrane with diameter of ≈ 1.5 μm under indenter load. More precisely, Lee with co-workers [16] experimentally documented the following mechanical characteristics of the graphene membrane in indenter test: the Young modulus $Y \approx 1$ TPa, the intrinsic strength $\sigma_{int} \approx 130$ GPa, and the fracture strain $\varepsilon_f \approx 0.25$.

In previous paragraph, values of the mechanical characteristics for bulk (large-area) graphene are presented which are obtained in the simulations [19] and the experiment [16]. Hereinafter, we will exploit these values for comparison with those simulated for graphene nanoribbons in order to quantitatively specify the size and edge effects exerted on the mechanical characteristics in such nanoribbons.

Zhao with co-workers [19] focused their simulations on elastic moduli of graphene nanoribbons having an approximately square shape with the diagonal length varying between 1.17 and 15.62 nm. The simulations were performed in two versions: by the molecular dynamics method with the AIREBO potential and by the orthogonal tight-binding (TB) method. With both these methods, it was revealed the trend that the Young modulus Y in armchair and zigzag directions gradually grows with rising the nanoribbon's diagonal length (Fig. 4a). For large enough values of the length, the Young modulus Y slowly converges to its values that characterize bulk graphene and are denoted as Y_b in Fig. 4a. In doing so, the molecular dynamics simulations demonstrated a pronounced chirality effect on Y whose values are different for tensile tests along armchair

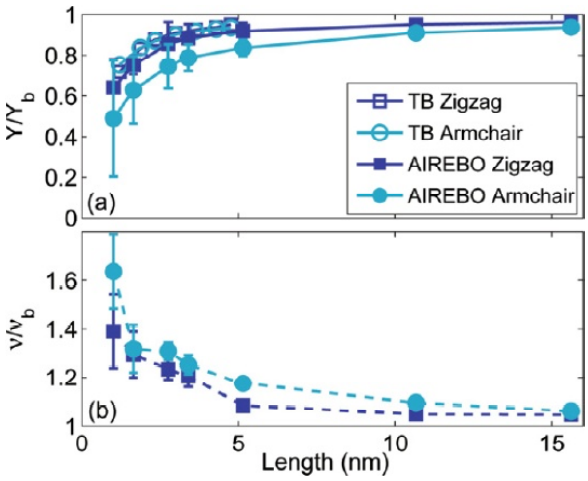

Fig. 4. Normalized Young modulus Y/Y_b (a) and normalized Poisson ratio ν/ν_b (b) as a function of nanoribbon diagonal length for uniaxial tension along the armchair and zigzag directions. Reprinted (adapted) with permission from [H. Zhao, K. Min, N.R. Aluru, Size and chirality dependent elastic properties of graphene nanoribbons under uniaxial tension. *Nano Letters*, Volume 9 (2009) 3012-3015]. Copyright (2009) American Chemical Society.

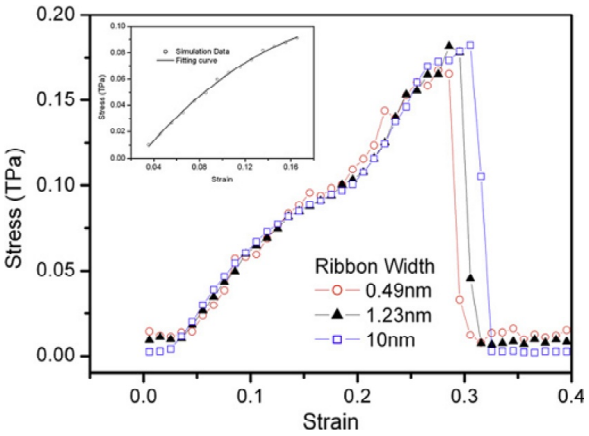

Fig. 5. Stress as a function of strain for (36,5), (36,11), (36.82) armchair graphene nanoribbons at 300K, which corresponds to the length of 7.6 nm and the widths of 0.49 nm, 1.23 nm, and 10 nm, respectively. The inset is the nonlinear fitting of the stress-strain curves for strain from 4% to 17%. Reprinted with permission from [H. Bu, Y. Chen, M. Zou, H. Yi, K. Bi, Z. Ni, Atomistic simulations of mechanical properties of graphene nanoribbons. *Physics Letters A*, Volume 373 (2009) 3359-3362]. Copyright (2009) Elsevier.

and zigzag directions (Fig. 4a). At the same time, according to simulation by the TB method, the chirality is in fact negligible (Fig. 4a).

Also, with the molecular dynamics method, it was revealed the trend that the Poisson ratio ν simulated in armchair and zigzag directions decreases when the nanorribbon's diagonal length increases (Fig. 4b) and slowly converges to its values that specify bulk graphene and are denoted as ν_b in (Fig. 4b). The chirality effect is pronounced for the Poisson ratio (Fig. 4b).

Bu with co-workers [20] utilized molecular dynamics method with the Tersoff potential in order to simulate deformation and fracture processes in graphene nanoribbons with various widths under tensile tests. The key aim of these simulations was to reveal the size and edge effects on tensile strength, fracture strain and Young modulus. The length of nanoribbons was chosen as 7.9 nm, and their widths were 0.49, 1.23, and 10 nm. In the simulations under consideration, graphene nanoribbons were subjected to tensile mechanical load along armchair direction at temperature of 300K [20].

With the molecular dynamics simulations, the stress-strain dependences were calculated (Fig. 5), for nanoribbons with various widths [20]. It was found that graphene nanoribbons are deformed in a typical brittle way without apparent plastic deformation (Fig. 5). The fracture occurs through successive

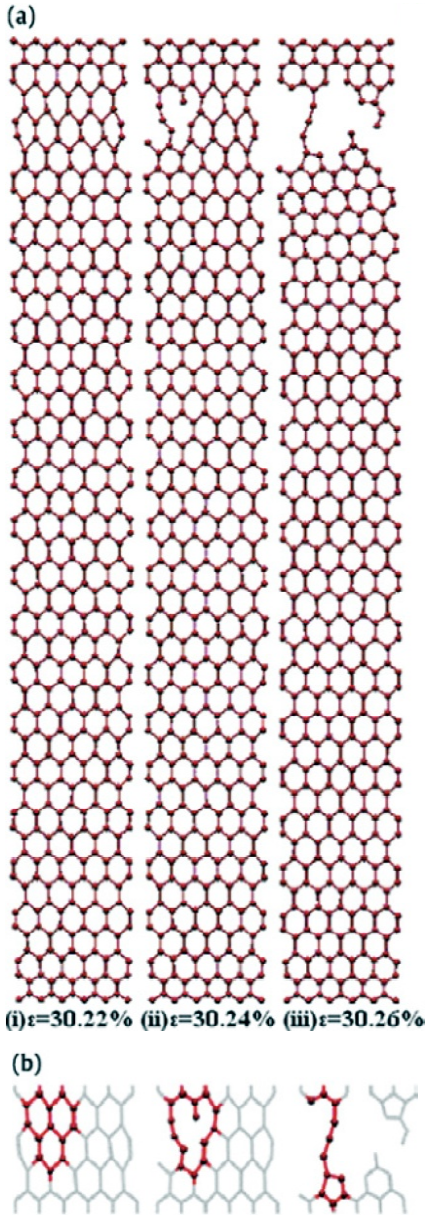

Fig. 6. The structural evolution and the fracture mechanism of the armchair graphene nanoribbons with the length of 7.6 nm and the width of 1.23 nm under tensile load. Reprinted with permission from [H. Bu, Y. Chen, M. Zou, H. Yi, K. Bi, Z. Ni, Atomistic simulations of mechanical properties of graphene nanoribbons. *Physics Letters A*, Volume 373 (2009) 3359-3362]. Copyright (2009) Elsevier.

breaks of carbon-carbon (C-C) atomic bonds and corresponding decrease in cross sectional area of the nanoribbon (Fig. 6). The tensile strength σ_t of nanoribbons has its values of around 170-175 GPa (Fig. 5), and these values are significantly higher than the intrinsic strength ($\sigma_{int} \approx 130$ GPa) experimentally documented [16] in the case of a circle-like graphene membrane with diameter of ≈ 1.5 μm under indenter load. The simulated values of the

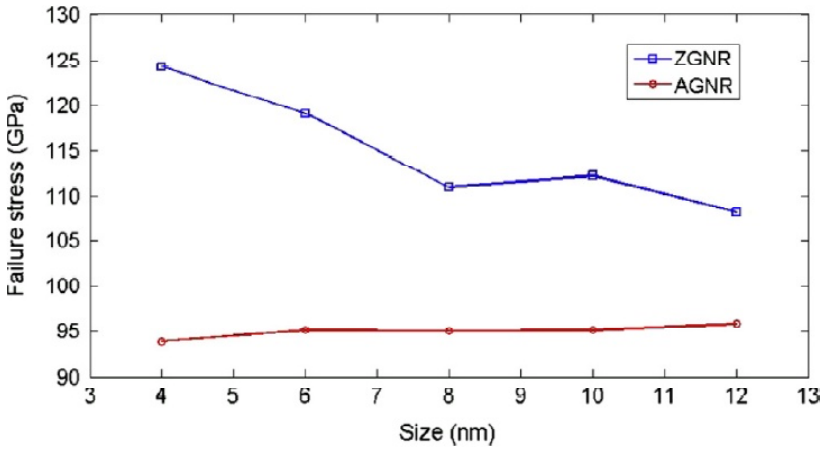

Fig. 7. Size effects for failure stress of square graphene nanoribbons. Reprinted with permission from [Y. Chu, T. Ragab, C. Basaran, The size effect in mechanical properties of finite-sized graphene nanoribbon. *Computational Materials Science*, Volume 81 (2014) 269-274]. Copyright (2014) Elsevier.

Young modulus Y are around 1.24 TPa [20]. The experiment [16] with the graphene membrane showed $Y \approx 1$ TPa. Besides, in the simulations [20], Bu with co-workers revealed that the fracture strain $\varepsilon_f \approx 0.3$, for the nanoribbons under consideration, whereas the experiment [16] gives $\varepsilon_f \approx 0.25$, for the graphene membrane.

Lu with co-workers [21] performed simulations focused on the edge, size and chirality effects on both the elastic properties of graphene nanoribbons and fracture mechanisms operating in them under quasistatic uniaxial tension. Classical molecular mechanics and molecular dynamics simulations based on the second-generation reactive empirical bond-order (REBO) potential have been utilized in description of deformation and fracture processes occurring in graphene nanoribbons. Also, a thermodynamics model has been suggested taking into consideration the edge, size and chirality effects on the Young modulus of graphene nanoribbons [21]. With these methods, Lu with co-workers revealed that the Young modulus increases, as the nanoribbon width increases for both the zigzag and armchair tension directions. In doing so, values of the Young modulus of a nanoribbon deformed along the zigzag tension direction are larger than those along the armchair tension direction.

With the simulations [21], fracture mechanisms in graphene nanoribbons were identified. It was found that fracture surfaces are typically zigzag ones [21], because the zigzag edge energy is lower than the armchair edge energy [22]. In particular, tension in the armchair direction initiates formation of a straight crack which generates at the nanoribbon edge and is perpendicular to the tension direction. When a graphene is under tension in the zigzag direction, a crack typically generates in the nanoribbon interior, and crack growth tends to occur along zigzag directions making 60° and -60° angles with the tension direction. These fracture mechanisms were observed in other simulations as well [18,23].

Chu with co-workers [23] focused their research efforts on the size effect in mechanical properties of graphene nanoribbons. With the molecular dynamics method based on the AIREBO potential, they performed simulations of uniaxial tension tests for nanoribbons with various sizes and aspect ratios. These simulations revealed interesting trends in sensitivity of mechanical characteristics of graphene nanoribbons to their shape, sizes and chirality. In particular, it was found that mechanical properties of graphene nanoribbons are sensitive enough to their sizes and shapes during tension in the zigzag direction, whereas the effects of nanoribbon sizes and shapes on these properties are low [23].

Let us discuss this and other trends. So, in the case of tension in zigzag direction, simulations of tension test for square-shaped graphene nanoribbons revealed that the Young modulus increases, while the fracture stress and strain decrease with rising the nanoribbon width from 4 to 12 nm (see, e.g., Fig. 7) [23]. At the same time, the size effect on mechanical characteristics of square-shaped graphene nanoribbons under tension in armchair direction is negligibly low (see, e.g., Fig. 7) [23]. In doing so, the maximum fracture stress for tension in the zigzag and armchair directions is 125.4 GPa and 103 GPa, respectively. The fracture strain for nanoribbons deformed in the zigzag and armchair directions is 0.2 and 0.14, respectively.

The discussed chirality effect on the mechanical characteristics is related to the specific features

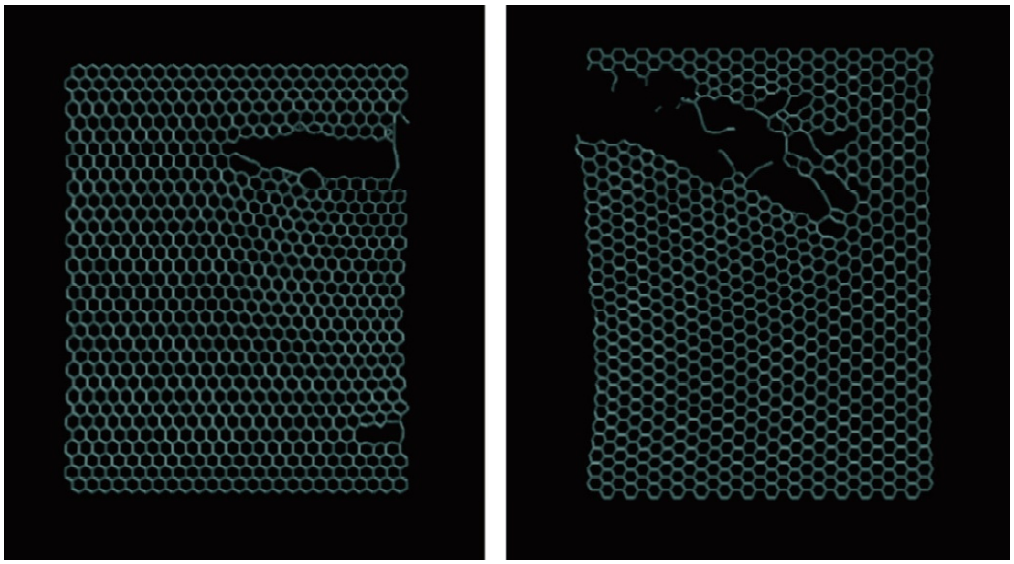

Fig. 8. Fracture of graphene nanoribbons under uniaxial tension. Reprinted with permission from [Y. Chu, T. Ragab, C. Basaran, The size effect in mechanical properties of finite-sized graphene nanoribbon. *Computational Materials Science*, Volume 81 (2014) 269-274]. Copyright (2014) Elsevier.

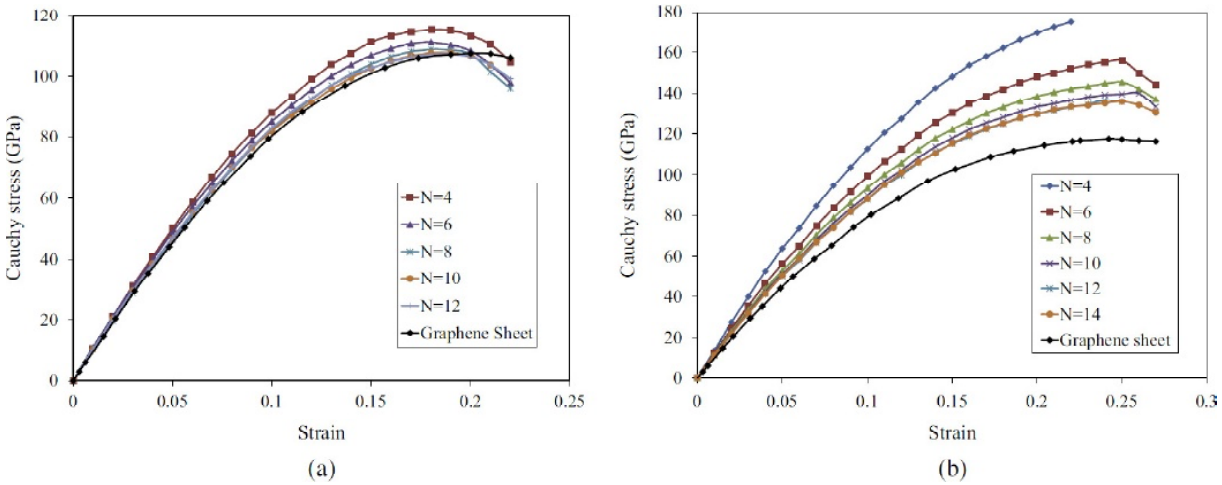

Fig. 9. The stress-strain curves for graphene nanoribbons with different widths. (a) Armchair nanoribbons and (b) zigzag nanoribbons. Reprinted with permission from [A. Tabarraei, S. Shadalou, J.-H. Song, Mechanical properties of graphene nanoribbons with disordered edges. *Computational Materials Science*, Volume 96 (2015) 10-19]. Copyright (2015) Elsevier.

of fracture micromechanisms operating in graphene nanoribbons. First, as with results presented in papers [18,21], the simulations [23] showed that fracture edges are predominantly zigzag-shaped (Fig. 8). Second, cracks are typically nucleated at edge and interior regions of graphene nanoribbons when they are deformed along armchair and zigzag directions, respectively [23]

Sensitivity of mechanical properties exhibited by graphene nanoribbons to aspect ratio characterizing their shapes was examined through simulations of tension tests for nanoribbons specified by the same length (12 nm) and various width values (2.4, 4, 6, 10, and 12 nm). For tension in the zigzag direction, it was found that the Young modulus increases, while the fracture stress and strain decrease with rising the nanoribbon width from 2.4 to 12 nm. In the case of tension in the armchair direction, the Young modulus increases, when the nanoribbon width increases. However, this trend is less-pronounced, as compared to tension in the zigzag direction. For tension in the armchair direction, the fracture stress and strain are weakly sensitive to the nanoribbon width. The maximum fracture stress for tension in the zigzag and armchair directions is around 130 GPa and 98 GPa, respectively. The maximum fracture strain for nanoribbons deformed in the zigzag and armchair directions is around 0.2 and 0.12, respectively.

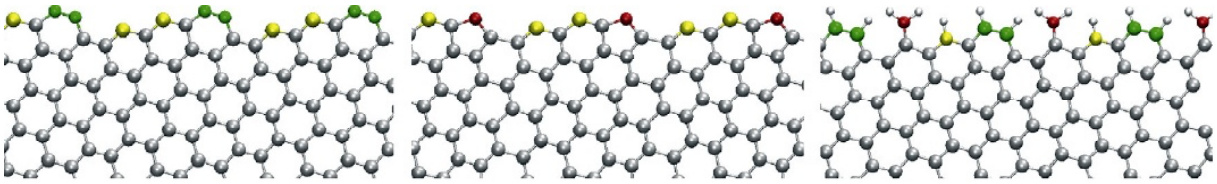

Fig. 10. (a) A chiral nanoribbon without any edge defect; zigzag atoms are shown in yellow and armchair atoms are shown in green, defects are generated by removing one of armchair atoms; (b) a nanoribbon with a pentagonal defect; (c) a nanoribbon with a Klein defect. The small grey atoms are hydrogen atoms (for details, see [18]). Reprinted with permission from [A. Tabarraei, S. Shadalou, J.-H. Song, Mechanical properties of graphene nanoribbons with disordered edges. *Computational Materials Science*, Volume 96 (2015) 10-19]. Copyright (2015) Elsevier.

Also, Chu with co-workers [23] performed simulations of tension tests for nanoribbons specified by the same width (2.5 nm) and various length values (5, 7.5, 10, and 12.5 nm). It was revealed that the aspect ratio effect on the mechanical characteristics (Young modulus, fracture stress and strain) of graphene nanoribbons with fixed length is rather small for tension in both the zigzag and armchair directions.

Tabarraei with co-workers [18] exploited density functional theory modeling in simulations of deformation and fracture processes occurring in graphene nanoribbons in tension tests. In doing so, size, chirality and edge effects on mechanical characteristics of graphene nanoribbons were revealed. Fig. 9 presents stress-strain dependences that specify graphene nanoribbons with various width values in the case of tensile deformation along the armchair and zigzag directions. The dependences show that the ultimate stress grows with decreasing the nanoribbon width, and this trend is more pronounced for tension in the zigzag direction. With the stress-strain curves presented in Fig. 9, Tabarraei with co-workers calculated the Young modulus as a function of the nanoribbon width. They found that, for both zigzag and armchair tension directions, the Young modulus increases with deceasing the nanoribbon width. This size effect is more pronounced in the case of deformation along the zigzag direction [18].

Fracture surfaces in graphene nanoribbons are typically zigzag ones. They make an angle of around 60^o and 90^o with the nanoribbon axis during tensile deformation tests along the zigzag and armchair directions, respectively [18]. Graphene tends to be fractured at its zigzag crystallographic surfaces, because the zigzag edge energy is lower than the armchair edge energy [22].

In most cases, computer simulations of deformation and fracture processes in graphene nanoribbons are concerned with nanoribbons having pure zigzag or armchair edges. Real graphene nanoribbons are fabricated as those having edges of a mixed geometry, that is, edges consisting of both zigzag and armchair segments. In doing so, the physical properties of graphene nanoribbons are sensitive to their chirality, in which case geometry of the nanoribbon edges can be utilized in tuning these properties. Mechanical properties of such nanoribbons with mixed edges (Fig. 3) were examined in the simulations [18]. The mixed edge geometry is characterized by an angle α between the edge line and the zigzag direction. Tabarraei with co-workers [18] simulated tensile tests of graphene nanoribbons specified by $\alpha = 10.89^o$, 13.90^o, 19.11^o, and 23.41^o (Fig. 3). It was revealed that the edge geometry significantly affects both fracture stress and strain characterizing graphene nanoribbons; for details, see [18].

Also, the simulations [18] were focused on the effects of defects – pentagons and Klein defects - located at nanoribbon edges (Fig. 10) on mechanical characteristics exhibited by graphene nanoribbons. In doing so, Klein defects represent dangling carbon bonds passivated by hydrogen atoms (Fig. 10c). A pentagon is a positive topological disclination creating high internal stresses [5,24]. Its presence at the graphene nanoribbon edge leads to screening of its stress fields by the edge. The simulations [18] showed that both the fracture stress and strain of graphene nanoribbons decrease due to the presence of pentagons and Klein defects at nanoribbon edges.

4. CONCLUDING REMARKS

To summarize, there is a difference between the key mechanical characteristics (fracture strength, Young modulus, and fracture strain) simulated for the graphene nanoribbons [18-21,23] and those

experimentally measured [16] in the case of a circle-like graphene membrane with diameter of ≈ 1.5 μm under indenter load. This difference and the simulation results themselves are indicative of the edge, size and chirality effects on deformation behaviors exhibited by graphene nanoribbons. In the simulations of Young modulus specifying graphene nanoribbons, the results [18] obtained by dense functional theory method are in conflict with those [19-21,23] revealed by the molecular dynamics approach. So, according to molecular dynamics simulations [19-21,23], the Young modulus increases with rising the nanoribbon width, whereas dense functional theory simulations [18] show the opposite trend. At the same time, both molecular dynamics [19-21,23] and dense functional theory simulations [18] indicate that the fracture strength decreases when the nanoribbon width increases. The strength ranges from 90 to 180 GPa, depending on the nanoribbon width and chirality. Also, in the simulations, the fracture strain is in the range from 0.12 to 0.30, depending on the nanoribbon width and chirality.

Besides, with the simulations [18,21,23], fracture mechanisms in graphene nanoribbons were identified (Fig. 8). It was recognized that fracture surfaces are typically zigzag ones [18,21,23], because the zigzag edge energy is lower than the armchair edge energy [22]. In particular, tension in the armchair direction initiates formation of a straight crack which generates at the nanoribbon edge and is perpendicular to the tension direction. When a graphene is under tension in the zigzag direction, a crack typically generates in the nanoribbon interior, and crack growth tends to occur along zigzag directions making 60^o and -60^o angles with the tension direction.

Finally, note that science on mechanical properties of graphene nanoribbons is in its infancy. Computer simulations absolutely dominate in this area. Their results (briefly presented in this review) are interesting and important for understanding the fundamentals of deformation and fracture processes occurring in graphene nanoribbons. At the same time, experimental verifications/corrections of computer simulation results are highly needed.

ACKNOWLEDGEMENTS

This work was supported by the Russian Science Foundation (Research Project 14-29-00199).

REFERENCES

[1] A. K. Geim and K. S. Novoselov // *Nature Mater*. **6** (2007) 183.
[2] A.H. Castro Nero, F. Guinea, N.M.R. Peres, K.S. Novoselov and A.K. Geim // *Rev. Mod. Phys*. **81** (2009) 109.
[3] A. A. Balandin // *Nature Mater*. **10** (2011) 569.
[4] F. Molitor, J. Guttinger, C. Stampfer, S. Droscher, A. Jacobson, T. Ihn and K. Ensslin // *J. Phys.: Condens. Matter* **23** (2011) 1.
[5] I.A. Ovid'ko // *Rev. Adv. Mater. Sci*. **30** (2012) 201.
[6] L.P. Biro and P. Lambin // *New J. Phys*. **15** (2013) 035024.
[7] I.A. Ovid'ko // *Rev. Adv. Mater. Sci*. **34** (2013) 1.
[8] M. Han, B. Ozyilmaz, Y. Zhang and P. Kim // *Phys. Rev. Lett.* **98** (2008) 206805.
[9] X. Li, X. Wang, L. Zhang and S. Lee, H. Dai // *Science* **319** (2008) 1229.
[10] Y. Wu, Y. Lin, A. Boi, K. Jenkins, F. Xia, D. Farmer, Y. Zhu and P. Avouris // *Nature* **472** (2011) 74.
[11] Y.-W. Son, M.L. Cohen and S. Louie // *Phys. Rev. Lett.* **97** (2006) 216803.
[12] V. Barone, O. Hod and G.E. Scuseria // *Nano Lett.* **6** (2006) 2748.
[13] S. Dutta, S. Lakshmi, S.K. Pati // *Phys. Rev*. *B* **77** (2008) 073412.
[14] M. Topsakal and S. Ciraci // *Phys. Rev*. *B* **81** (2010) 024107.
[15] L.-H. Qu, J.-M. Zhang, K.-W. Xu, V. Ji // *Physica E* **56** (2014) 55.
[16] C. Lee, X. Wei, J.W. Kysar and J. Hone // *Science* **321** (2008) 385.
[17] D.S.L. Abergel, V. Apalkov, J. Berashevich, K. Ziegler and T. Chakraborty // *Adv. Phys.* **59** (2010) 261.
[18] A. Tabarraei, S. Shadalou and J.-H. Song // *Comput. Mater. Sci.* **96** (2015) 10.
[19] H. Zhao, K. Min and N.R. Aluru // *Nano Lett.* **9** (2009) 3012.
[20] H. Bu, Y. Chen, M. Zou, H. Yi, K. Bi and Z. Ni // *Phys. Lett. A* **373** (2009) 3359.
[21] Q. Lu, W. Gao and R. Huang // *Modelling Simul. Mater. Sci. Eng.* **19** (2011) 054006.
[22] M. Xu, A. Tabarraei, J. Paci, J. Oswald and T. Belytschko // *Int. J. Fract.* **173** (2012) 163.
[23] Y Chu, T. Ragab and C. Basaran // *Comput. Mater. Sci*. **81** (2014) 269.
[24] I.A. Ovid'ko // *Rev. Adv. Mater. Sci*. **34** (2013) 12.